

Utah State University

DigitalCommons@USU

---

International Symposium on Hydraulic Structures

---

May 17th, 1:30 PM

## Experimental Analysis on a Low Crested Rubble Mound Breakwater

I. Martone

*University of Naples Federico II, ivo.martone@unina.it*

K.A. Galani

*University of Patras, kgalani@upatras.gr*

P. Gualtieri

*University of Naples Federico II, paola.gualtieri@unina.it*

C. Gualtieri

*University of Naples Federico II, carlo.gualtieri@unina.it*

A.A. Dimas

*University of Patras, adimas@upatras.gr*

Follow this and additional works at: <https://digitalcommons.usu.edu/ishs>

---

### Recommended Citation

Martone, I. (2018). Experimental Analysis on a Low Crested Rubble Mound Breakwater. Daniel Bung, Blake Tullis, 7th IAHR International Symposium on Hydraulic Structures, Aachen, Germany, 15-18 May. doi: 10.15142/T39S6B (978-0-692-13277-7).

This Event is brought to you for free and open access by the Conferences and Events at DigitalCommons@USU. It has been accepted for inclusion in International Symposium on Hydraulic Structures by an authorized administrator of DigitalCommons@USU. For more information, please contact [digitalcommons@usu.edu](mailto:digitalcommons@usu.edu).



## Experimental Analysis on a Low Crested Rubble Mound Breakwater

*I. Martone*<sup>1</sup>, *K.A. Galani*<sup>2</sup>, *P. Gualtieri*<sup>1</sup>, *C. Gualtieri*<sup>1</sup> & *A.A. Dimas*<sup>2</sup>

<sup>1</sup>*Department of Civil, Architectural and Environmental Engineering, University of Naples Federico II, Naples, Italy*

<sup>2</sup>*Department of Civil Engineering, University of Patras, Patras, Greece*

*E-mail: ivo.martone@unina.it*

**Abstract:** *In the present study, the flow induced by waves around a physical model of a detached low crested rubble mound breakwater is investigated experimentally. The model was designed with a scale factor of 1/30, parallel to the shoreline, along a coast of constant slope 1/15, assuming Froude similarity to be valid. For the design of the rock armour layer, the van der Meer's hydraulic stability formula was applied. Two wave conditions were examined: one with an offshore wave height of 2 m (Case A) and another with the maximum annual characteristic offshore wave height (Case B) calculated in prototype scale. The measurements include surface elevation time series as well as three-dimensional velocity time series of the flow around the model. The results include flow patterns on the seaward and leeward side of the breakwater for both wave conditions as well as transmission and reflection coefficients. Along the leeward side, the current profiles have an offshore direction close to the bottom and a shoreward direction close to the free surface where the reduction of the water depth induced an acceleration of the flow and is influenced by the overtopping. Transmission and reflection coefficient's data are compared with that from existing literature. The comparison revealed that literature equations tended to underestimate the transmission coefficient due to the critical condition represented by a zero free-board breakwater, whereas it overestimates the reflection coefficient, possibly due to the fact that these formulae were obtained from experiments performed with emerged breakwaters.*

**Keywords:** *Shore protection, low-crested breakwater, experimental analysis, ADV, transmission/reflection coefficient.*

### 1. Introduction

The function of a rubble mound breakwater is to protect a coastal area from wave attack and shoreline scour. Shore-parallel, detached, and segmented breakwater's configurations are used for shore protection. These structures have their crest at/or below the mean water level and the term 'rubble' as used here includes rock, riprap and precast concrete armour units. Coastal structures with a low crest are called 'low-crested breakwaters' and they allow some wave transmission behind themselves by generating wave-breaking.

First experimental studies on three-dimensional physical models were carried out on emerged structures by Gourlay (1974), Mory and Hamm (1997), and Chapman et al. (2000) to study flow circulation and wave setup. Further experiences were obtained on low-crested breakwaters on irregular wave conditions by Ruol and Faedo (2002) and Zanuttigh and Lamberti (2006) within the framework of the EU-funded project DELOS. Most of the experiments are aimed to transmit and reflect phenomena or to formulate new empirical stability formulas. However, studying flow currents around the breakwaters helps with understanding structure behaviour.

Few velocity laboratory measurements are available and the majority were performed with non-realistic physical models such as submerged steps, narrow models fixed in flume basin or small scale models affected by turbulence. Comparisons between experimental analysis and numerical simulations use few laboratory data (Losada 2005) or suffer model limitations (Garcia et al. 2004). Flow pattern analysis around an isolated breakwater was performed by Sutherland et al. (2000) and recent experiments are under investigation to understand zero freeboard breakwater hydrodynamics (Martone, MSc Thesis, 2016; Ballas, MA Thesis, 2016). Notably, in this configuration the water circulation generated by the crest may influence bed morphodynamics. The wave interaction with low-crested breakwater depends on the wave conditions and wave attack direction. However, the design must be accurate in order to ensure the proper function of a submerged or low-crested structure. Another big challenge is the crest freeboard design: many studies show the influence of crest width on wave transmission coefficient (Seabrook and Hall 1998). Thus, experiments on a zero freeboard rubble-mound breakwater were conducted under monochromatic wave conditions to improve knowledge of hydrodynamics around such a particular coastal structure as well as wave reflection and transmission studying.

The present paper is structured in three parts. First of all, the laboratory setup and the physical model construction are presented. Second, the methods used for the post-processing of time-averaged velocity and wave height data are

---

described. Finally, the observed flow patterns are discussed and the measured transmission and reflection coefficients are compared to literature predictive formulas.

## 2. Experimental setup

The experimental measurements were carried out in the Hydraulic Engineering Laboratory of the Department of Civil Engineering, University of Patras (Greece). The experiments took place inside the wave basin which had a surface area of 12 x 7 m and water depth of 1.05 m. The basin was equipped with a DHI paddle wave-maker that reproduced monochromatic, spectral or recorded waves produced by existing time series. A slope of 1/15 was installed inside the basin made by industrial anodised aluminum poles used to support stainless aluminum plates, 5 mm thick. The sloping beach was bounded by vertical aluminum plates creating a region narrower (4 m wide) than the wave basin (7 m wide).

The low-crested breakwater model was designed assuming Froude similarity for a geometrical scale of 1:30. Given a return period of 50 years for the significant wave height  $H_s$  at the toe of the breakwater, the physical model was designed through the van der Meer's formula (1990): the nominal diameter,  $D_{n50}$ , of the armour layer, consisting of two rows of rocks supported by a steel frame, was obtained as follows:

$$\frac{h'_c}{h} = (2.1 + 0.1 S) e^{-0.14 N_s^*} \quad (1)$$

$$N_s = \frac{H_s}{D_{n50} \Delta}; N_s^* = N_s S_p^{-\frac{1}{3}} \quad (2)$$

where  $S$  is the damage level;  $h'_c$  is the structure height;  $h$  is the water depth;  $S_p$  is the wave steepness obtained with peak wave;  $\Delta$  is the relative buoyant density and  $N_s^*$  is the spectral stability number. A value of 1.21 m was obtained for the  $D_{n50}$ . Afterwards, a sample of 1514 rocks was collected and weighed in the laboratory. The nominal diameter was given by the following equation:

$$D_n = \left( \frac{W}{\gamma_r} \right)^{1/3} \quad (3)$$

where  $W$  is the weight of the rock and  $\gamma_r$  is the specific weight of the rocks assumed as 2.63 g/cm<sup>3</sup>. In the end, the  $D_{n50}$  was found and the results are shown in Table 1.

**Table 1.** Nominal diameter and mean weight differences between prototype and physical model.

| TITLE            | Prototype | Model  |
|------------------|-----------|--------|
| $D_{n50}$ (m)    | 1.19      | 0.0396 |
| $D_{n15}$ (m)    | 1.10      | 0.0368 |
| $D_{n85}$ (m)    | 1.34      | 0.0445 |
| Mean weight (kg) | 4428      | 0.164  |
| Grading (-)      | 1.2       | 1.2    |

Two wave conditions were considered for a total amount of 124 ten-minute long generated time series, with a wave height of 2 m (Case A) and with the maximum annual characteristic wave height (Case B), in prototype scale.

Free surface elevations were recorded in six different locations along the direction of wave propagation using wave gauges (Type 202, DHI) (Figure1) which measure conductivity between two parallel electrodes partly immersed into water and whose accuracy was 1 mm.

An Acoustic Doppler Velocimeter was placed in eight locations (hereafter referred to as stations) along the two slope toes to collect velocity data. The ADV system consisted of a 16-MHz Micro ADV probe (Sontek/YSI, 2002) with three side-looking acoustic receivers and one acoustic transmitter (Figure 1). The sampling volume was approximately  $0.3 \text{ cm}^3$  and it was located 5 cm from the acoustic transmitter. The instrument resolution was about 0.01 cm/s, while its accuracy was of the order of 1% of measured velocity. The sampling rate was 50 Hz.

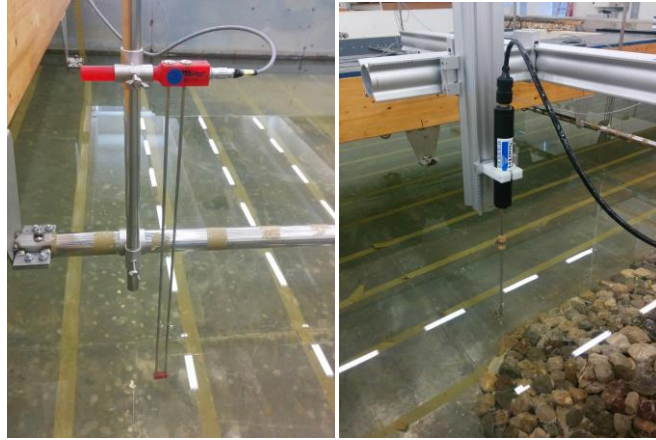


**Figure 1.** From the left to the right: the wave gauge Type 202 from DHI and Acoustic Doppler velocimeter (ADV).

Four of the ADV stations were located at the seaward toe of the model and four at the shoreward one (Figure 2). The first array was placed along the centerline of the model, while the second, the third and the fourth ones were set, respectively, at 80 cm, 133 cm and 160 cm from the centerline. In each station, velocity measurements were performed in several points along the flow depth with the first point located one centimeter from the bottom: the number of recorded points per station depends on breaking or no-breaking wave conditions. For surface elevation measurements, seven wave gauges were placed along the physical model centerline (Table 2).

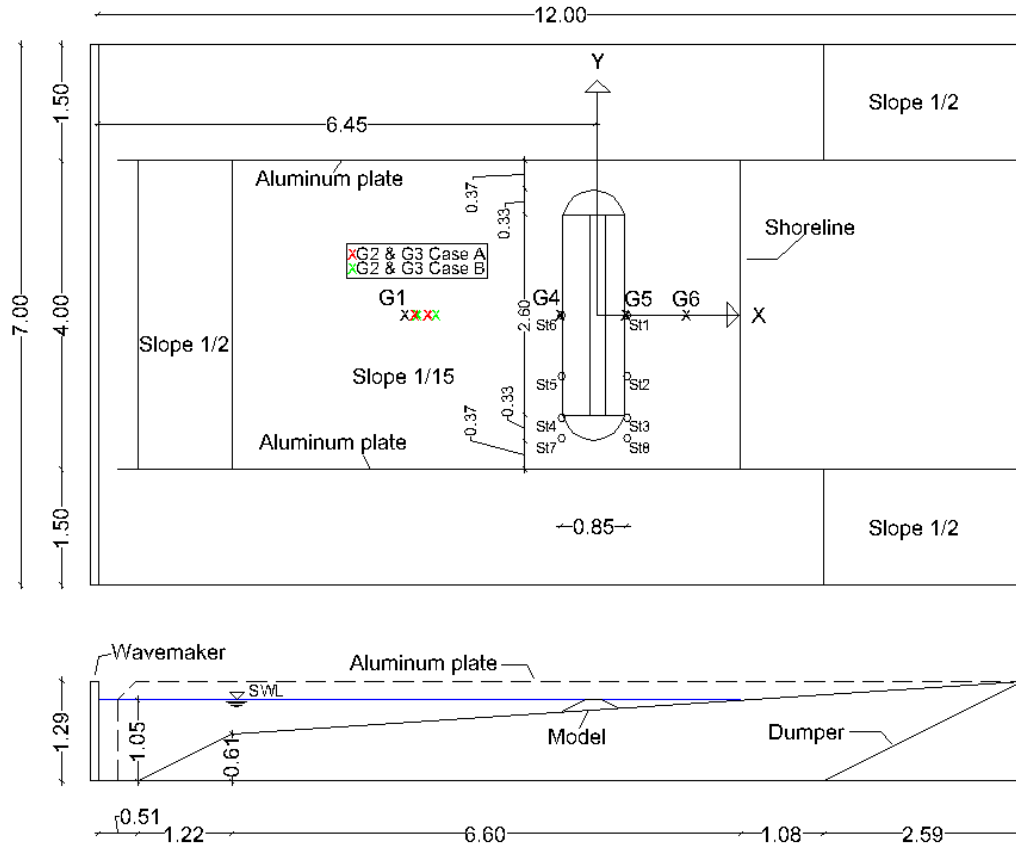


Figure 2. Wave basin sketch.

Table 2. Stations and wave gauges positions (coordinates system showed in Figure 3).

| Station | Station Location |       | Recorded Points | Wave gauge | Case A | Case B |
|---------|------------------|-------|-----------------|------------|--------|--------|
|         | X (m)            | Y (m) |                 |            | (m)    | (m)    |
| (-)     | X (m)            | Y (m) | (-)             | (-)        | (m)    | (m)    |
| 1       | 0.40             | 0.00  | 6               | G1         | -2.27  | -2.27  |
| 2       | 0.40             | 0.80  | 6               | G2         | -2.15  | -2.11  |
| 3       | 0.40             | 1.33  | 5               | G3         | -1.97  | -1.87  |
| 4       | -0.40            | 1.33  | 10              | G4         | -0.47  | -0.47  |
| 5       | -0.40            | 0.80  | 10              | G5         | 0.37   | 0.37   |
| 6       | -0.40            | 0.00  | 10              | G6         | 1.15   | 1.15   |
| 7       | -0.40            | 1.60  | 9               | /          | /      | /      |
| 8       | 0.40             | 1.60  | 6               | /          | /      | /      |

### 3. Data post-processing

The surface elevation time series were analyzed using the MIKE Zero-WS Wave Analysis Toolbox developed by DHI in order to estimate the reflection and transmission coefficients, while velocity measurements were analyzed using a

Matlab code to obtain mean velocity profiles. For spurious spikes in time series, a de-spiking method was used for the outliers. A typical ADV time series gives instantaneous velocity components during the wave cycle. In order to get the mean velocity, the instantaneous velocities were time averaged using the following equations:

$$U_i = \frac{1}{N_p} \sum_{j=1}^{N_p} u_{ij} \quad (4)$$

$$U = \frac{1}{N} \sum_{i=1}^N U_i \quad (5)$$

where  $U$  is the period-averaged velocity;  $u_{ij}$  is the instantaneous velocity of the  $j$ -frame of the  $i$ -cycle;  $U_i$  is the mean velocity of the  $i$ -cycle;  $N_p$  is the number of recorded frames per cycle ( $N_p = 46$  in Case A and 56 in Case B); and  $N$  is the number of recorded cycles ( $N = 300$  in this study) over which average value was performed.

The reflection coefficient, which is the partial wave reflection caused by breakwater roughness and permeability, was obtained through the MIKE-Reflection Analysis Module which calculates the incident and reflected wave spectrums and the average reflection coefficient. The frequency domain separation handles concurrent recordings from several wave gauges as it solves the governing equations by use of at least squares fit approach. The basic method is described by Mansard and Funke (1980) and extended by Zelt and Skjelbreia (1992). The coefficient is defined as:

$$C_r = \frac{H_r}{H_i} \quad (6)$$

The Mansard and Funke methodology proposes that for monochromatic waves the gauges spacing should lie in the range:

$$X_{12} = \frac{\lambda}{10}; \frac{\lambda}{6} < X_{13} < \frac{\lambda}{3}; X_{13} \neq \frac{\lambda}{5}; X_{13} \neq \frac{3\lambda}{10} \quad (7)$$

where  $\lambda$  is the wave length at the depth where the gauges were placed;  $X_{12}$  and  $X_{13}$  are the spacings between G1 and G2, and G1 and G3, respectively. Therefore, according to Eq. (7), the new gauges spacings were:

$$X_{12} = 0.1 \lambda_{G1}; X_{23} = 0.15 \lambda_{G1} \quad (8)$$

where  $\lambda_{G1}$  is the wave length at  $d = 0.30$  m (wave gauge G1);  $X_{23}$  is the distance between G2 and G3. On the other hand, the transmission coefficient, defined as the percentage of wave energy passing through and over the breakwater, is calculated as the ratio of the incident wave height recorded at the front toe and the wave height recorded at the back toe of the breakwater: the zero-up crossing method was adopted for the analysis. For this method, a wave is defined as the portion of a record between two successive crossings of zero level uphill. A sample of four time series has been selected for the analysis: in this way, the accuracy of the coefficient was verified comparing multiple experiments.

The first step was to calculate the incident wave height at the front toe of the low-crested breakwater model. Since the wave height measured by the front gauge includes both the incident and the reflected wave, the incident wave height

was calculated by subtracting the reflected wave from the measured one using the reflection coefficient according to the equation:

$$H_i = \frac{H_{measured}}{1 + C_r} \quad (9)$$

The second step was to calculate the transmitted wave height at the leeward side of the submerged breakwater. Existing formulas define the transmitted wave height as:

$$H_{t,m0} = 4 \sqrt{m_0} \quad (10)$$

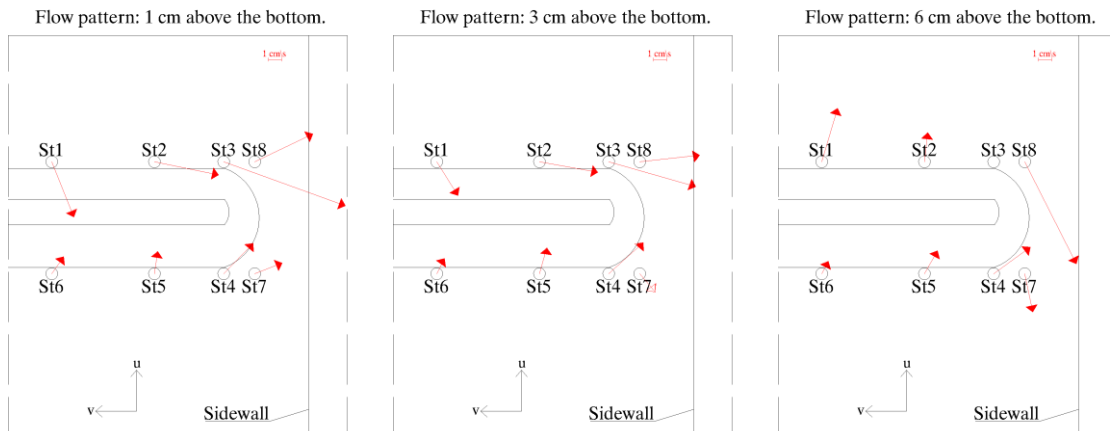
where  $m_0$  is the zero-th spectral moment, so the transmission coefficient was obtained as shown below:

$$C_t = \frac{H_{t,m0}}{H_i} \quad (11)$$

## 4. Results

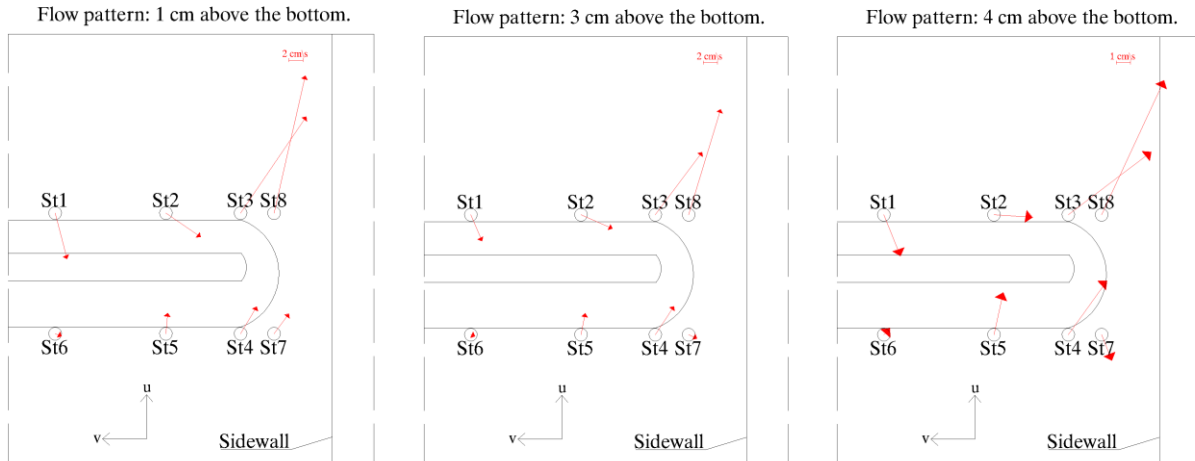
### 4.1. Time-Averaged Velocity Profiles

Figure 3 presents the velocity vectors at the eight stations and for three different depths for wave case A. Four stations were located at the front toe of the model and other four in the back toe of the breakwater. In the leeward side, after the wave breaking, big values of velocity components were found with opposite direction to the wave propagation. In the shoreward stations, a large negative  $V$  component towards the external side of the breakwater and a positive value of  $U$  close to the free surface that decreased down to negative velocities (directed to the offshore) near the bottom were observed. The  $W$  component was always positive suggesting a circular path of the particles. This trend appears completely different in the seaward stations where velocity components were found to be directed towards the shore.



**Figure 3.** Case A flow patterns at different depths from bottom.

Regarding Case B (Figure 4), the  $U$  component acquires positive values close to the surface (due to overflow) and negative ones close to the bottom (therefore directing back to the deep water). The  $V$  component was negative and, as in Case A, shows a current directing along the edge of the breakwater. The  $W$  component suggested a particle path directed to the free surface level. Nearby the gap, the  $U$  component changed its sign showing large positive values from the bottom to the surface while the  $V$  component was negative and larger close to the seabed. The  $W$  component was negative and increased towards the bottom.



**Figure 4.** Case B flow patterns at different depths from bottom.

#### 4.2. Reflection and Transmission Coefficients

The experimental values for the reflection coefficients were compared with those from literature equations, such as those from Seelig (1983), Postma (1989), Zanuttigh and van der Meer (2006) and Zanuttigh and van der Meer (2008) (Table 3). Results of least squares fit approach are shown in (Table 5). For the validation of the transmission coefficient, five experimental formulas were considered: van der Meer (1990), van der Meer and Daemen (1994), D'Angremond et al. (1996), Seabrook and Hall (1998) and Calabrese et al. (2002) (Table 4).

**Table 3.** Reflection coefficient formulas used in this study.

| AUTHOR                            | FORMULA   | PARAMETERS                             | COMMENTS   |
|-----------------------------------|---|--|--|
| (Seelig 1983)                     | $C_r = \frac{a \cdot \xi_0^2}{b + \xi_0^2} \quad (12)$              | $0.64 < a < 0.80$<br>$8.85 < b < 10$   | The values of the coefficients a and b change for armour units, rock permeable and impermeable slopes.   |
| (Postma 1989)                     | $C_r = 0.15 \cdot \xi_0^{0.73} \quad (13)$                          | $0.64 < a < 0.96$<br>$4.80 < b < 9.64$ | The wave period has influence on the reflection behaviour, so $\xi_0$ introduces some scatter.   |
| (Zanuttigh and van der Meer 2006) | $C_r = \tan(a \cdot \xi_0^b) \quad (14)$                            | $0.12 < a < 0.16$<br>$0.87 < b < 1.47$ | It reproduce different slope types; physical bounds and gives a relationship with the roughness.   |
| (Zanuttigh and van der Meer 2008) | $C_r = C_{r(eq14)} \cdot (0.67 + 0.37 \frac{R}{H_{mo}}) \quad (15)$ | $-1 < \frac{R_c}{H} < 0.5$             | It takes into account low-crested breakwaters through the relative crest free-board $R_c/H$ . $R_c = 0$ represents the zero freeboard condition. |



**Table 4.** Transmission coefficient formulas used in this study.

| AUTHOR                         | FORMULA   | PARAMETERS   | COMMENTS   |
|--------------------------------|---|--|--|
| (van der Meer 1990)            | $C_t = -0.31 \frac{R_c}{H_{m0}} + 0.46$ (16)  | $0 < C_t < 1$  | Coefficient linearly decreases with relative crest freeboard $R_c/H_{m0}$ .  |
| (van der Meer and Daemen 1994) | $C_t = a \frac{R_c}{D_{n50}} + b$ (17)  | $a = 0.031 \frac{H_i}{D_{n50}} - 0.24$<br>$b = -5.42s_{op} + 0.0323 \frac{H_i}{D_{n50}} - 0.0017 \left(\frac{B}{D_{n50}}\right)^{(1.84)}$                      | The influence of the crest width is included to explain the behaviour of $C_t$ if $R_c = 0$ .  |
| (D'Angremond et al. 1996)      | $C_t = -0.4 \frac{R_c}{H_i} + 0.64 \left(\frac{B}{H_i}\right)^{(-0.31)} \cdot \left(1 - e^{-0.5\xi}\right)$ (18)  | $0.12 < a < 0.16$<br>$0.87 < b < 1.47$   | It includes the influence of the non-dimensional crest freeboard, $R_c/H_i$ , the wavelength $Lop$ and the crest width $B$ .                   |
| (Seabrook and Hall 1998)       | $C_t = 1 - \left[ e^{-0.65 \frac{R_c}{H_{moi}} - 1.09 \left(\frac{H_{moi}}{B}\right)} + 0.047 \left(\frac{B \cdot R_c}{L \cdot D_{n50}}\right) - 0.067 \left(\frac{H_{moi} \cdot R_c}{B \cdot D_{n50}}\right) \right]$ (19) | $5 \leq B/H_{moi} \leq 74.47$<br>$0 < B(-R_c)/L \cdot D_{n50} < 7.08$<br>$0 < H_{moi}(-R_c)/B \cdot D_{n50} < 2.14$  | Design formula whose application is restricted to submerged structures.  |
| (Calabrese et al. 2002)        | $C_t = a \frac{R_c}{D_{n50}} + b$ (20)  | $a = (0.6957 \frac{H_{moi}}{h_c} - 0.7021) \cdot e^{0.2568 \frac{B}{H_{moi}}}$<br>$b = (1 - 0.562 \cdot e^{-0.0507\xi_0}) \cdot e^{-0.0854 \frac{B}{H_{moi}}}$ | Predictive expression based on large-scale tests resembling the formula by van der Meer and Daemen (1994) by substituting $D_{n50}$ with $B$ . |

The comparison between measured values and empirical formulas is shown in Figure 5 even though the dataset results are quite few. The line inside the graph represents full agreement. For the reflection coefficient, the Zanuttigh and van der Meer (2006) formula, designed for submerged breakwaters exclusively, presents the best fit with the reflection coefficient estimated above for Case A. However, a scatter is visible when comparing with the other formulas, though the values are concentrated in a small range. In Case B, the discrepancy between predicted and measured values is smaller than in Case A as far as it concerns Seelig (1983), Postma (1989) and Zanuttigh and van der Meer (2008) formulas.

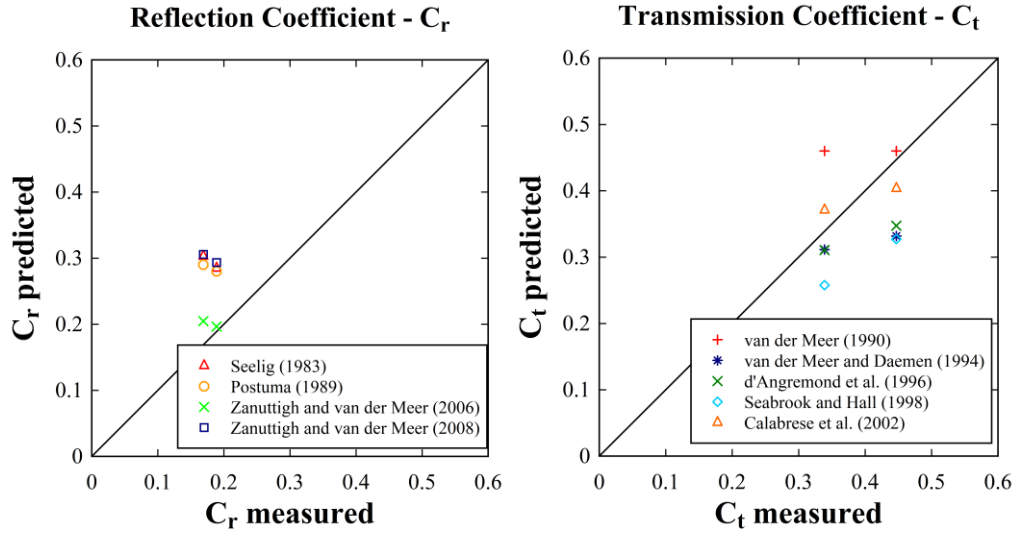


**Figure 5.** Reflection and transmission coefficient: comparison between predicted and measured values.

With respect to the reflection coefficient, the transmission coefficient presents larger scattering. The van der Meer (1990) formula does not give confidence in the measured results due to the zero freeboard condition. The largest discrepancy was given by van der Meer and Daemen (1994) formula. The Calabrese et al. (2002) formula, though it gives the best fit, appears out of validity range due to the Irribarren number which is defined as follows:

$$\xi_0 = \frac{\tan \vartheta}{(H_{m0t}/L_0)^{1/2}} \quad (21)$$

where  $H_{m0t}$  is the significant wave height at the structure toe,  $\tan \vartheta$  the front slope and  $L_0$  the offshore wave length.

**Table 5.** Mean values of reflection and transmission coefficients.

| Case A |       | Case B |       |
|--------|-------|--------|-------|
| $C_r$  | $C_t$ | $C_r$  | $C_t$ |
| (-)    | (-)   | (-)    | (-)   |
| 0.189  | 0.339 | 0.169  | 0.447 |

## 5. Conclusions

In this study, experiments on a zero freeboard rubble-mound breakwater were conducted under regular wave conditions in order to improve the knowledge of hydrodynamics around such coastal structures. A total number of 124 time series were generated. The physical model of a breakwater was built in a wave basin above a constant coastal slope of 1/15. The armour layer of the breakwater consisted of two rows of rocks supported by a steel frame.

The physical model performed well, showing very interesting comparisons between the well-known experimental formulas and measured values. As far as it concerns the reflection coefficient, it was found that the literature equations tend to overestimate its value, possibly due to the fact that these formulas were obtained by experiments performed with emerged breakwaters. As for the transmission coefficient, an underestimation given by the existing formulas was revealed due to the critical condition represented by a zero freeboard breakwater. It was seen that half of the wave energy was dissipated in both wave conditions by the seaward slope.

The potentially vulnerable regions were identified in the shoreward toe of the structure and close to the gap. Flow patterns on the seaward and leeward sides were observed for both wave conditions. With reference to Case A, along the leeward side, the current profiles had an offshore direction close to the bottom and an inshore direction close to

the free surface where the reduction of the water depth induces an acceleration of the flow, influenced by the overtopping.

A similar behaviour was observed for Case B, even though in station 3 negative mean velocity close to the bottom suggests the generation of an inshore current in contrast to the leeward current profiles.

In the seaward side, an inshore weak current was present in all stations. As mentioned above, the mean water level, increasing in the leeward zone due to the overtopping, induced a hydraulic gradient and, therefore, a return flow directing offshore. In emerged breakwaters, this return flow hinders the onshore transport associated with wave non-linearity and wave breaking and gives rise to a mean current directing offshore.

## 6. Acknowledgements

The first author acknowledges the support from the Erasmus Program 2015/2016. The second and fourth authors acknowledge the support of the research project 'ARISTEIA I-1718' implemented within the framework of the program 'Education and Lifelong Learning' and co-financed by the European Union (European Social Fund) and Hellenic Republic funds. Collaboration with staff of the Hydraulic Laboratory of the Civil Engineering Department of the University of Patras (Greece) is gratefully acknowledged.

## 7. References

- Calabrese, M., Vicinanza, D., and Buccino, M. (2002). "Large-scale experiments on the behaviour of low-crested and submerged breakwaters in presence of broken waves." *Proc. of the 28th Int. Conf. on Coastal Engineering, Cardiff, World Scientific*, 1900-1912.
- Chapman, B., Ilic, S., Simmonds, D., and Chadwick, A. (2000). "Physical model evaluation of the hydrodynamic produced around a detached breakwater scheme." In: Losada (Ed.), *Coastal Structures '99*. Balkema, 803-812.
- Garcia, N., Lara, J.L., and Losada, I.J. (2004). "2-D numerical analysis of near-field flow at low-crested permeable breakwaters." *Coast. Eng.*, 51 (10), 991-1020.
- Gourlay, G. (1974). "Wave set-up and wave generated currents in the lee of a breakwater or a headland." *Proc. Coastal Eng.*, 74, 1976-1995.
- Losada, I., Lara, J.L., Damgaard, E., and Garcia, N. (2005). "Modelling of velocity and turbulence fields around and within low-crested rubble-mound breakwaters." *Coast. Eng.*, 52, 867-885.
- Mansard, E.P.D., and Funke, E.R. (1980). "The measurement of incident and reflected spectra using a least squares method." *ICCE '80*, Sydney, Australia, 154-172.
- Mory, M., and Hamm, L. (1997). "Wave height, setup and current around a detached breakwater submitted to regular or random wave forcing." *Coast. Eng.*, 31, 77-96.
- Palmer, G. N., and Christian, C.D. (1998). *Design and Construction of Rubble Mound Breakwaters*. Tech.rep.
- Postma, G.M. (1989). "Wave reflection from rock slopes under random wave attacks." PhD Thesis, Delft University of Technology.
- Ruol, P. and Faedo, A. (2002). "Physical model study on low-crested structures under breaking wave conditions." *Proc. V MED-COAST Workshops on Beaches of the Mediterranean and Black Sea*, Turkey, E. Ozhan (Editor), 83-96.
- Seabrook, S.R., and Hall, K.R. (1998). "Wave Transmission at Submerged Rubble-mound Breakwaters." In: *Coastal Engineering Proceedings; No 26 (1998): Proc. of 26th Conference on Coastal Engineering*, Copenhagen, Denmark.
- Seelig, N.W. (1983). "Wave reflection from coastal structure." *Proc. of Conference on Coastal Structures*, ASCE, Arlington.
- Sutherland, J., Whitehouse, R.J.S., and Chapman, B. (2000). "Scour and deposition around a detached rubble-mound breakwater." In: Losada (Ed.), *Coastal Structures '99*. Balkema, 897-904.
- Tomasichio, G.R., and D'Alessandro, F. (2013). "Wave energy transmission through and over low crested breakwaters." In: *Proceedings 12th International Coastal Symposium (Plymouth, England)*, *Journal of Coastal Research*, Special Issue 65, 398-403, ISSN 0749-0208.

- van der Meer, J. W. (1990). Data on Wave Transmission Due to Overtopping. Tech. rep, Delft Hydraulics, Report No. H986, prepared for CUR C67.
- van der Meer, J. W. (1995). Conceptual Design of Rubble Mound Breakwaters. Tech. rep, TU Delft.
- van der Meer, J. W. and Daemen, I.F.R. (1994). "Stability and wave transmission at low crested rubble mound structures." *Journal of Waterway, Port, Coastal and Ocean Engineering*, 1, 1-19.
- Zanuttigh, B., and van der Meer, J.W. (2006). "Wave reflection from Coastal Structures." *Proc. of 30<sup>th</sup> International Conference on Coastal Engineering*, ASCE, San Diego, California, USA.
- Zanuttigh, B., and van der Meer, J.W. (2008). "Wave reflection from coastal structures in design conditions." *Journal of Coastal Engineering*, 55, 771-779.